This copy of the ESI replaces the previous version published on 30-Sep-2021.

Supplementary Information for

Local Kondo-Scattering in 4*d*-electron RuO_x Nanoclusters on Atomically-Resolved Ultrathin $SrRuO_3$ Films

Chuangye Song,[1,2‡] Tao Bo,[1,2‡], Xin Liu,[3] Pengjie Guo,[1,2] Sheng Meng,[1,2,4*] Kehui Wu,[1,2,4*]

[1]Songshan Lake Materials Laboratory, Dongguan, Guangdong 523808, China

[2]Institute of Physics, Chinese Academy of Sciences, Beijing 100190, China

[3]Swiss Light Source, Paul Scherrer Institute, Villigen 5232, Switzerland

[4]School of Physics, University of Chinese Academy of Sciences, Beijing 100049, China

Corresponding author: smeng@iphy.ac.cn; khwu@iphy.ac.cn;

[‡]These authors contributed equally to this work.

This copy of the ESI replaces the previous version published on 30-Sep-2021.

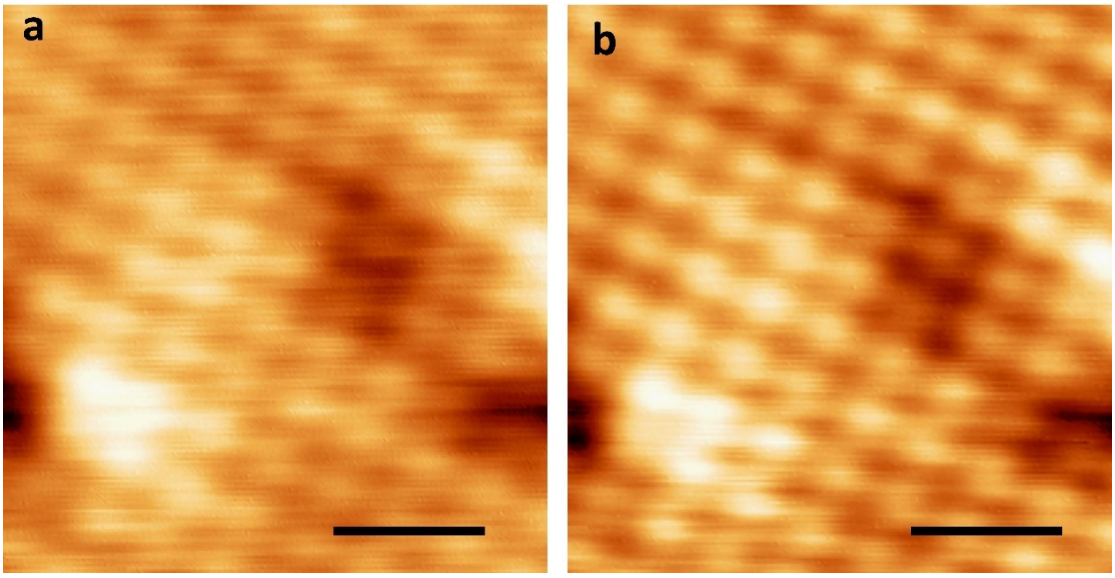

Figure S1. Sample-bias dependent STM images. STM images measured at the same location with sample bias V_b= -500 mV (a) and V_b= -50 mV (b), I_t = 200 pA. Scale bar is 1 nm.

This copy of the ESI replaces the previous version published on 30-Sep-2021.

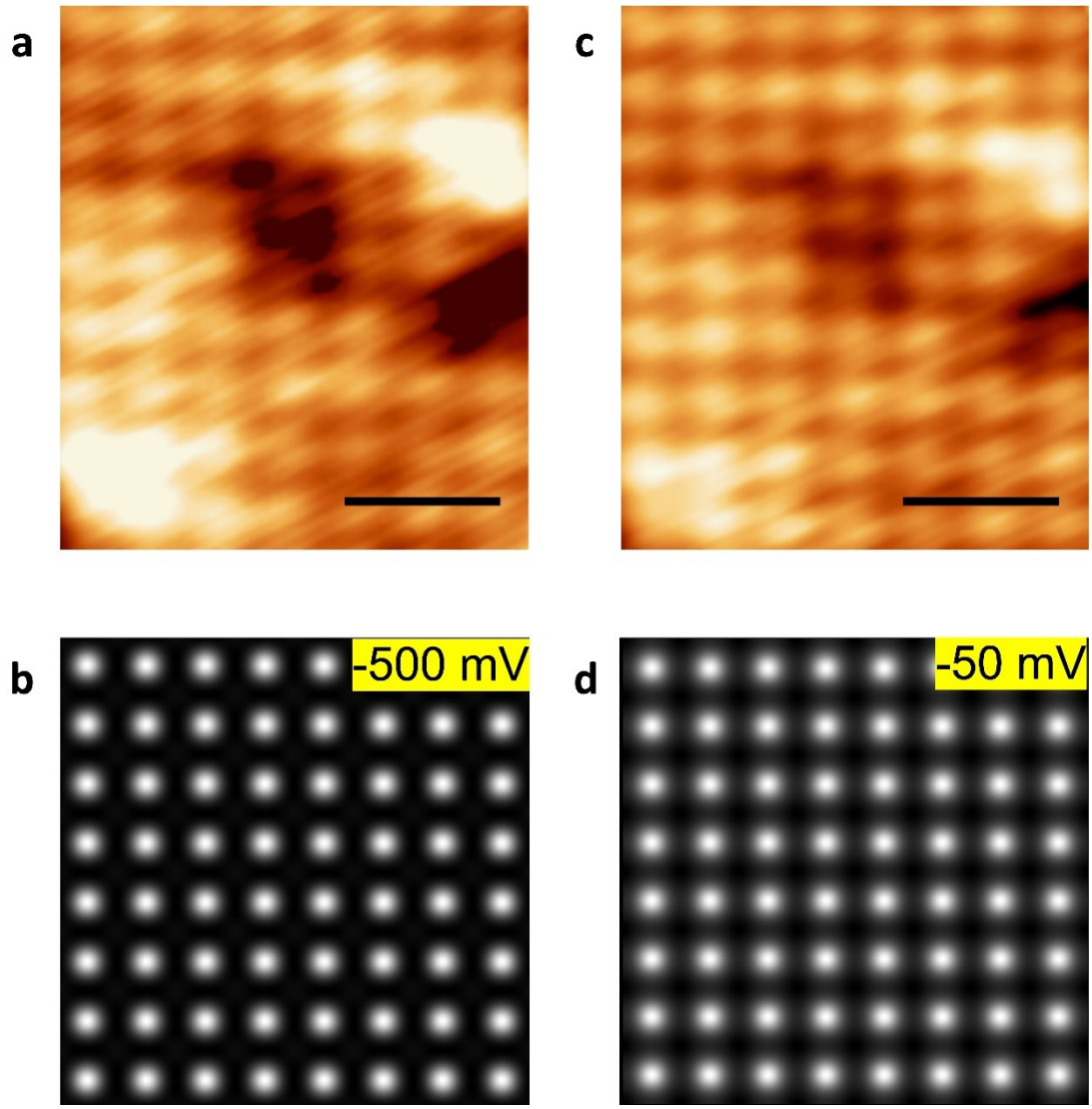

Figure S2. Experimental (a) and calculated (c) STM images with V_b=-500 mV. Experimental (b) and calculated (d) STM images with V_b=-50 mV. Scale bar is 1 nm.

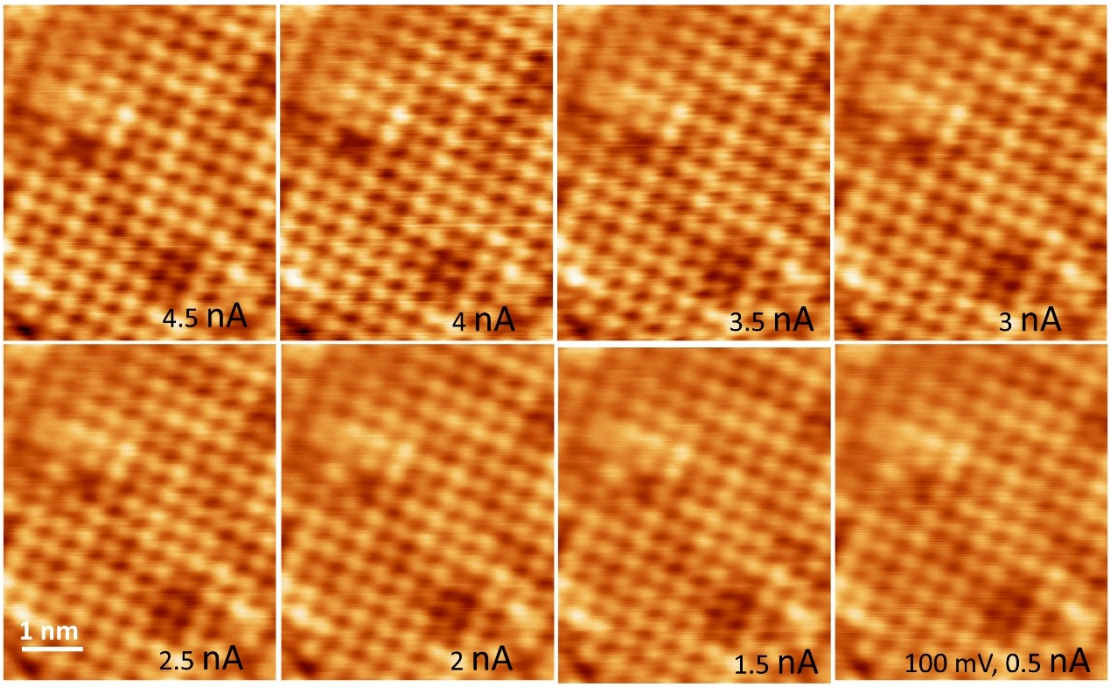

Figure S3. Tip-sample-distance dependent STM images. STM images measured at the same location with V_b= 100 mV fixed, I_t varies from 0.5 nA to 4.5 nA, no atomic arrangement change is observed.

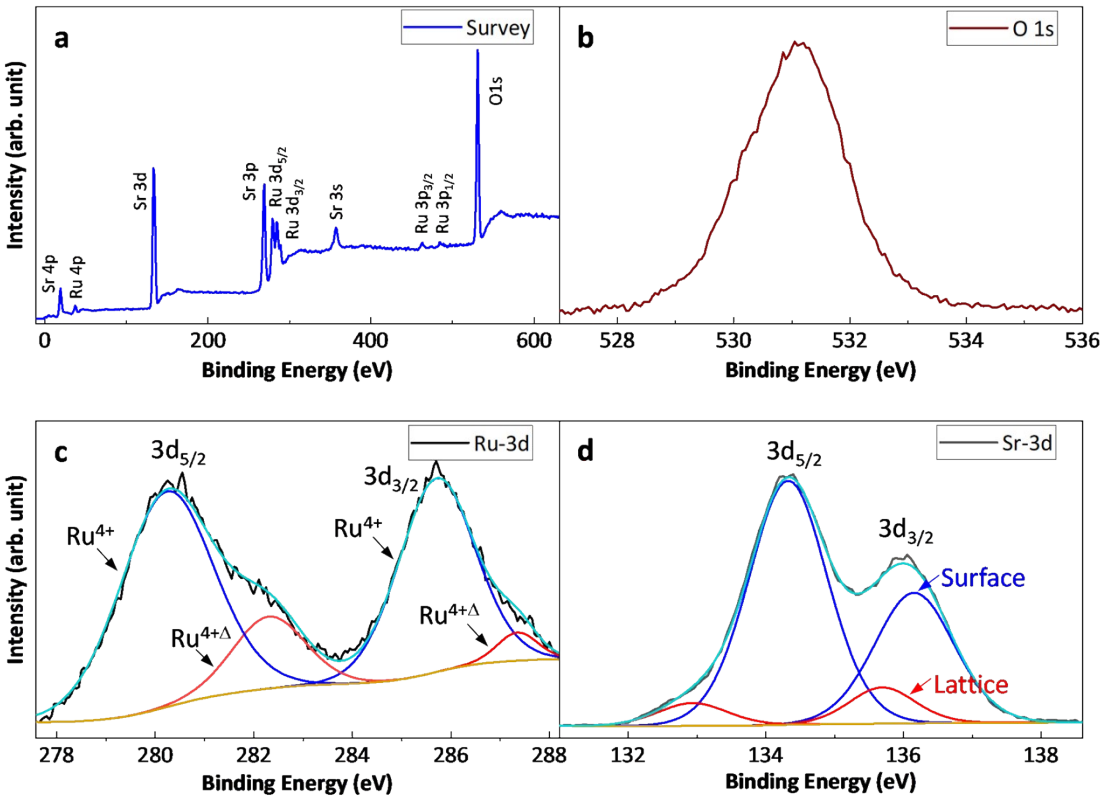

Figure S4. Surface composition analysis. (a) Grazing incidence X-ray photoelectron spectroscopy of the surface chemical composition of ultrathin $SrRuO_3$ thin film. (b) O 1s XPS spectrum. (c) Ru-3d XPS spectrum. (d) Sr-3d XPS spectrum.

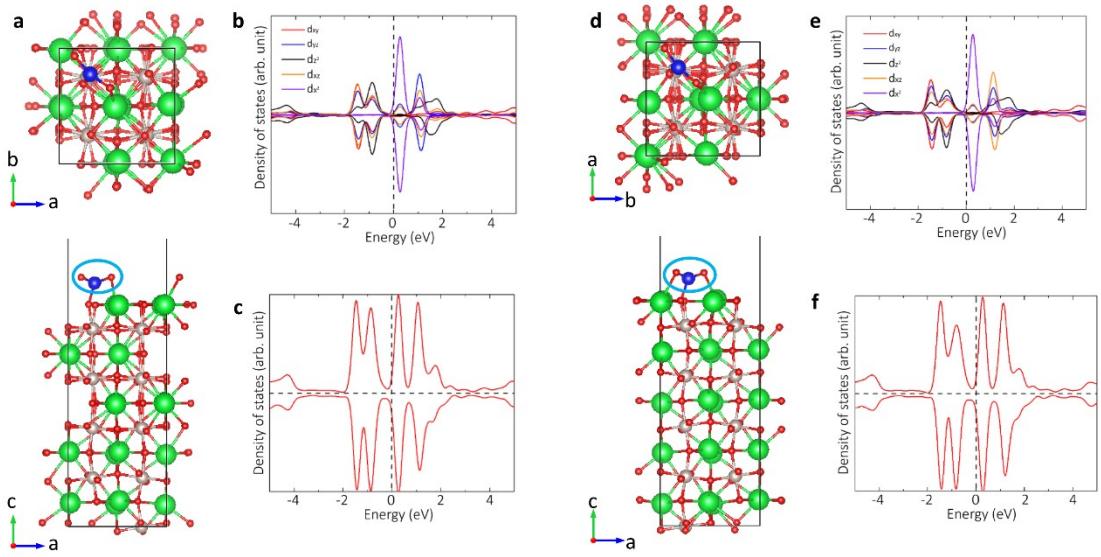

Figure S5. DFT calculations. (a) Top and side views of the optimized structure model for RuO_x-SRO adsorption system. Here we use blue atom to denote the adsorbed Ru (dashed circle). The PDOS (b) of the adsorbed Ru atom and the total DOS (c) of adsorbed Ru atom, with 4*d*-orbital-resolved $e_g(d_{xy},d_{yz},d_{xz})$ and $t_{2g}(d_{x^2},d_{z^2})$ bands. (d) Top and side views of the optimized structure model for another RuO_x-SRO adsorption system. The PDOS (e) of the adsorbed Ru atom and the total DOS (f) of adsorbed Ru atom, with 4*d*-orbital-resolved $e_g(d_{xy},d_{yz},d_{xz})$ and $t_{2g}(d_{x^2},d_{z^2})$ bands. In both cases, spin-down states were filled more than the spin-up states near the E_F, and thus the net magnetization is produced. The Sr, Ru and O atoms in the bulk are denoted with green, grey and red spheres, respectively.

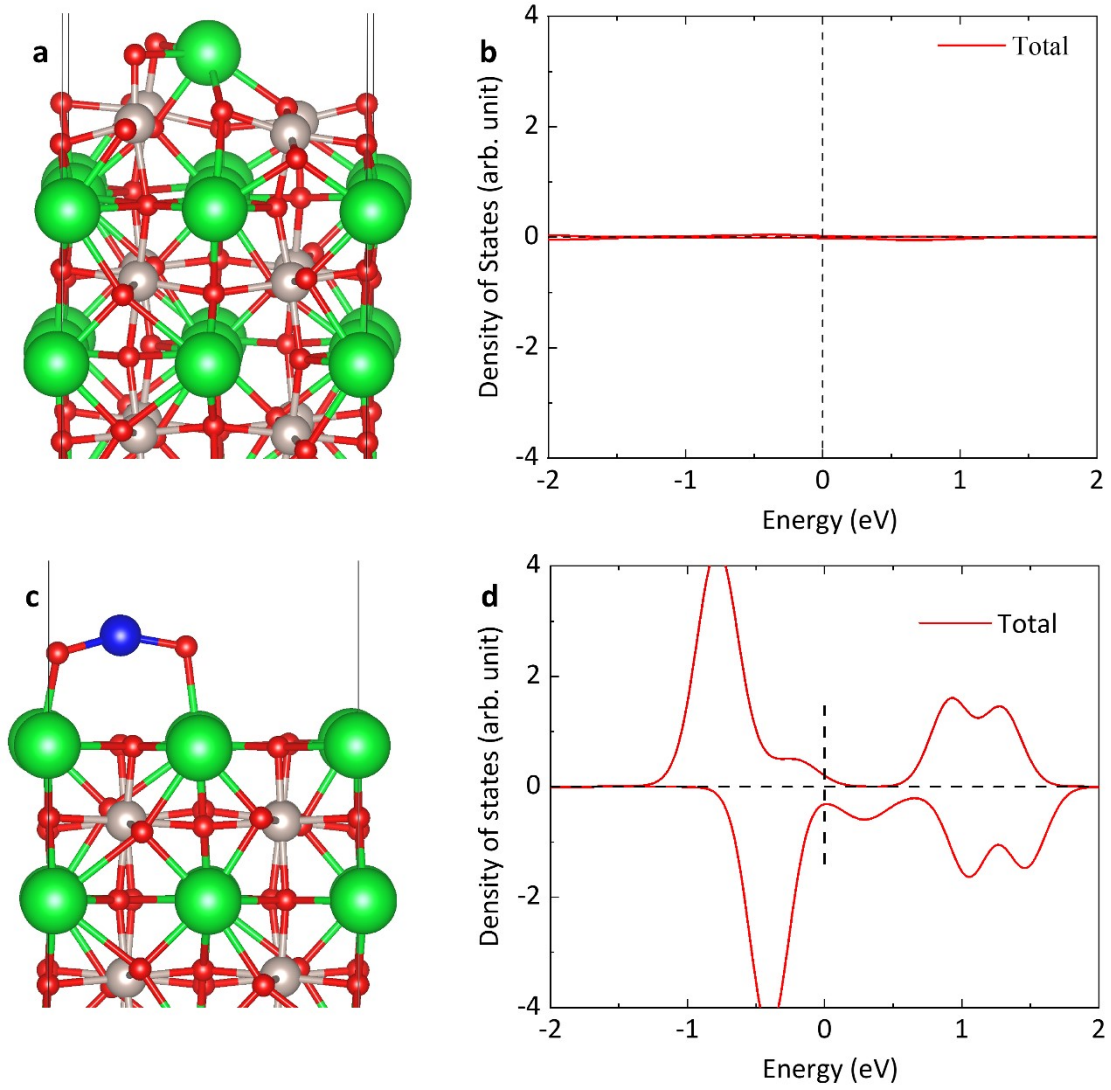

Figure S6. (a) Side view of the optimized structure model for SrO_x-$SrRuO_3$ adsorption system. (b) The total PDOS of adsorbed Sr atom. (c) Side view of the optimized structure model for RuO_x-$SrRuO_3$ adsorption system. Here we use blue atom to denote the adsorbed Ru. (d) The total PDOS of adsorbed Ru atoms. The Sr, Ru and O atoms in the bulk are denoted with green, grey and red spheres, respectively.

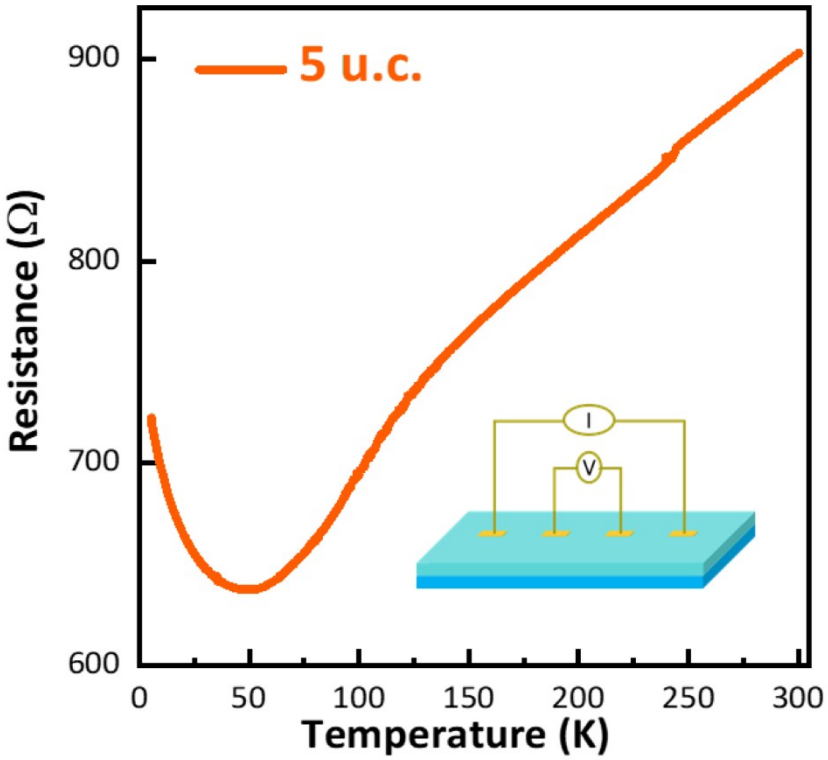

Figure S7. Temperature-dependent resistance. The inset is the schematic of four-probe method. T_K ~ 50 K can be revealed.